

COMPUTATIONAL MODELING FOR THE COUPLING ROD-ANODE IN ALUMINUM INDUSTRY

(1) Adriano G. Batista; (1) Fábio A. Cunha; (2) M. Sena

(1) Departamento de Engenharia Mecânica, Centro Tecnológico, Universidade Federal do Pará - UFPA. Rua Augusto Corrêa, Guamá. Belém – PA – Brasil. CEP: 66075-110. e-mail: fabioalfaia@yahoo.com.br

(2) Instituto de Estudos Superiores da Amazônia - IESAM. Av. Gov. José Malcher, 1148. Nazaré. Belém-PA/ Brasil. CEP: 66055-260. e-mail: mjssena@iesam.com.br

Abstract

In the production of aluminum, the reduction in the electrolysis cell is the most demanding phase in energy. The anode of this cell is produced by the Albras. It is composed by coque and pitch, which is used as an agglutinate. To be transported and immersed in the cell, they need to be coupled to an aluminum rod by a yoke. The geometry of the coupling will dictate its electric conduction, dissipation and mechanical strength characteristics. The rod-anode set presents symmetry in relation to two axes. So, just a quarter of the original geometry is modeled. This work will describe a finite element model of the anode, including the yoke and the rod. Electric, thermal and structural analyses are performed using an indirect coupling technique. The results are then discussed and the next steps of the work are presented.

Keywords: *finite elements, aluminum, anode, rod, coupling*

1. INTRODUCTION

The problem studied in this work is the analysis of the coupling rod-anode, used in the reduction process of the aluminum industry. This set is subjected to electrical, thermal and mechanical loadings. This type of problem can be solved using numerical procedures, like the finite element method. In fact, the finite element analysis is successfully used in problems dealing with complex geometries and loadings (Batoz, 1995 and Bathe, 1996).

Dupuis(1998) reviews the advantages and disadvantages of 2D and 3D models for modeling aluminum reduction cell. The author has also developed a 1D thermal model to reproduce dynamic cell behavior and to give answer to “what if” question. (Dupuis and Tabh, 1992).

Vogelsang et al (1997) discuss magneto-hydrodynamic simulations in an aluminum cell using a 3D finite element ANSYS model. Their purpose was to demonstrate improvements in cell stability and performance. Obtained by the modernization of the Rheinwerk plant.

Sherbinin et al (2000) developed software using 2D and 3D models for cell optimization and the development of new designs. They developed software for various processes, like: thermo-electric fields; influence of design parameters on energy regime; simulation of the case when gas formations of different shapes and form are present on the surface and gas-hydrodynamic processes.

The software Ansys was used to perform the finite element analysis in this work. The model can be used to analyze different configurations for the coupling rod-anode. This procedure can lead to savings in the energy consumed.

The Albras – Alumínio Brasileiro S.A., located in the Pará State uses 615 MW in electric power, being one of the greatest consumers in Brazil. Albras contributed to this academic work allowing the authors to access data associated to their anode production line.

The rod-anode coupling is composed by two distinct materials: the rod is built in aluminium and the anode is composed by a mix of coque and pitch. The interface between the two materials is made of cast iron. The electrical, thermal and mechanical loads influence each other. In other words, they are coupled.

During the reduction process, an electric current passes through the rod and anode. Heat is generated during this process, by the Joule Effect. The loss of electric potential in the process is the heat generated per unit volume. A temperature distribution is then verified in the anode body due to this effect. This temperature distribution causes thermal stresses that will be combined to the weight of the set to define the mechanical stresses acting in the structure.

The rod is used to insert and to remove the anode to and from the electrolytic cell. It also drives the electrical current to the anode. The complete unit is shown in Fig. 1.

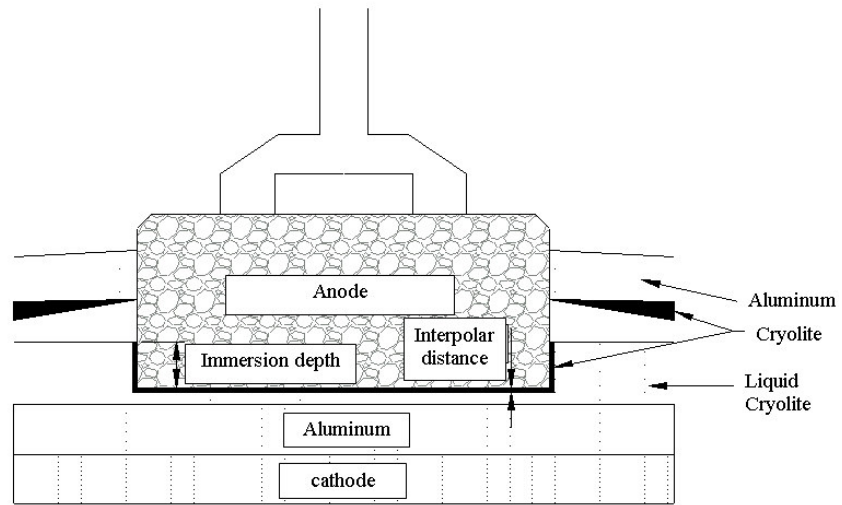


Figure 1. Set rod-anode used in the aluminum industry.

2. MODELING CONSIDERATIONS

In this section, the main quantities calculated by the finite element method will be briefly described. Each analysis will be considered: mechanical, thermal and electrical.

2.1. MECHANICAL AND THERMAL STRESSES

The static stresses that will be calculated in the structural analysis are of two types: mechanical and thermal. They will be discussed in this section.

The relations between stress and strain are described by the Eq. 1.:

$$\{\sigma\} = [D]\{\varepsilon\} \quad (1)$$

Where:

$$\{\sigma\} = \left[\sigma_x \quad \sigma_y \quad \sigma_z \quad \sigma_{xy} \quad \sigma_{xz} \quad \sigma_{yz} \right]^T - \text{Stress vector}$$

$$[D] = \text{Elastic matrix (in the case of linear behaviour).}$$

$$\{\varepsilon\} = \left[\varepsilon_x \quad \varepsilon_y \quad \varepsilon_z \quad \varepsilon_{xy} \quad \varepsilon_{xz} \quad \varepsilon_{yz} \right]^T - \text{Deformation vector}$$

In the case of thermal stresses, these relations take the form of Eq. 2:

$$\{\sigma\} = [D]\{\varepsilon^{el}\} \quad (2)$$

Where:

$$\{\varepsilon^{el}\} = \{\varepsilon\} - \{\varepsilon^{th}\}$$

$$\{\varepsilon\} = \left[\varepsilon_x \quad \varepsilon_y \quad \varepsilon_z \quad \varepsilon_{xy} \quad \varepsilon_{xz} \quad \varepsilon_{yz} \right]^T - \text{Deformation vector}$$

$$\{\varepsilon^{th}\} - \text{Thermal deformation vector}$$

In the three-dimensional case, the thermal deformations are given by Eq. 3.

$$\{\varepsilon^{th}\} = \Delta T \begin{bmatrix} \alpha_x & \alpha_y & \alpha_z & 0 & 0 & 0 \end{bmatrix}^T \quad (3)$$

Where:

α_x - Thermal expansion coefficient in the x direction

$\Delta T = T - T_{REF}$

T - Temperature

T_{REF} - Reference temperature (without deformation)

The principal stresses (σ_1, σ_2 e σ_3) are given by the cubic expression in Eq. 4.

$$\begin{vmatrix} \sigma_x - \sigma_0 & \sigma_{xy} & \sigma_{xz} \\ \sigma_{xy} & \sigma_y - \sigma_0 & \sigma_{yz} \\ \sigma_{xz} & \sigma_{yz} & \sigma_z - \sigma_0 \end{vmatrix} = 0 \quad (4)$$

Where:

σ_0 - principal stress (3 values)

The Von Mises stress (σ_e) is a scalar parameter very often used in the mechanical analysis of structures. It is defined by the Eq. 5.

$$\sigma_e = \left(\frac{1}{2} \left[(\sigma_1 - \sigma_2)^2 + (\sigma_2 - \sigma_3)^2 + (\sigma_3 - \sigma_1)^2 \right] \right)^{\frac{1}{2}} \quad (5)$$

2.2. ELECTRICAL POTENTIAL

In steady-state conditions, the equation (6) gives, in cartesian coordinates, the electric potential in the structure, provided the boundary conditions.

$$\frac{\partial}{\partial x} \left(\frac{1}{\rho_x} \frac{\partial \Phi}{\partial x} \right) + \frac{\partial}{\partial y} \left(\frac{1}{\rho_y} \frac{\partial \Phi}{\partial y} \right) + \frac{\partial}{\partial z} \left(\frac{1}{\rho_z} \frac{\partial \Phi}{\partial z} \right) = 0 \quad (6)$$

Where:

Φ - Electric potential

2.3. HEAT GENERATION BY THE JOULE EFFECT

The electrical current that passes through the rod-anode set causes heat generation by the Joule Effect. If $\{J\}$ is the electric current density and $\{E\}$ is the potential difference, the application of the Ohm's Laws leads to the Eq.7.

$$\{J\} = [\rho]^{-1} \{E\} \quad (7)$$

The heat generated by the Joule Effect is used to calculate the power loss per unit volume. This power loss can be used as input data to a thermal analysis to find the temperature distribution due to the electrical current.

2.4 TEMPERATURE DISTRIBUTION

The Eq. 9 is the general form of the Heat Diffusion equation, in cartesian coordinates. In this work it was assumed that the thermal properties of the materials were isotropic, the thermal conductivity was constant and the process was in steady-state conditions.

$$\nabla^2 T = -\frac{Q}{k} \quad (9)$$

Onde:

T - is the temperature.

Q - is the energy per unit volume rate.

k - is the thermal conductivity.

3. INDIRECT COUPLED ANALYSIS

The coupling method used in this work was an indirect one. In this case, different data bases and files are constructed for each analysis. The analysis are done separately. The results obtained by one analysis are used as boundary conditions to the next one.

This type of coupling is applied when the analysis can be considered weakly coupled. To know if an analysis can be considered weakly coupled or not, the cause-effect relationships must be analysed and, if the results of one analysis do not influence considerably the others, the indirect approach can be used.

The Fig. 2 shows the basic flow-chart for an indirect coupled analysis. Each database contains the adequate finite element model. In the case of the software used, the meshes must have the same nodes and elements.

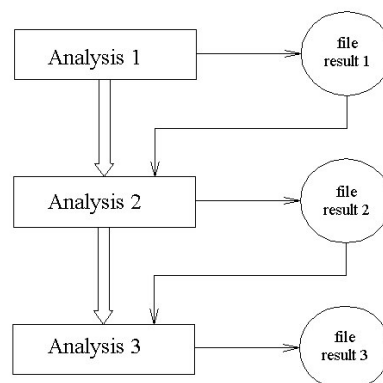


Figure 2. Flow-chart for an indirect coupled analysis.

The Ansys finite elements used in this work are shown in table 1. They are three-dimensional, with linear interpolation functions.

Table 1. Finite elements used in this work.

Structural analysis	Thermal analysis	Eletrical analysis
SOLID 45	SOLID 70	SOLID 69

3.1 GEOMETRY OF THE ROD-ANODE COUPLING

The CAD model of the rod-anode set is shown in Fig. 3. To simplify the model, the symmetry was considered and only one quarter of the geometry was used in the calculations. To do so, some degrees of freedom are fixed at the symmetry planes (Cook, 1989).

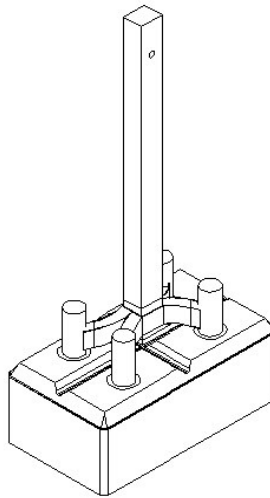


Figure 3. CAD 3D drawing of the rod-anode set.

3.2. MATERIAL PROPERTIES

The physical properties of the rod, the anode and the cast iron interface are shown in table 2 (these data were furnished by ALBRAS).

Tabela 2. Material properties.

Material properties	Rod (Aluminium AA 6106)	Anode (pitch and coque)	Interface (cast iron)
Elastic modulus (GPa)	7	4.5	207
Specific weight (kg/m ³)	7850	1650	7850
Poisson's ratio	0.33	0.1	0.29
Thermal conductivity (J/ C)	210	3.54	50
Electrical resistivity (Ω mm)	3,0E-5	5.13E-2	1.69E-4
Volumetric expansion coefficient	23 E-6	4.0E-6	1.51E-5

3.3. FINITE ELEMENT MESH

The finite element mesh was of free type (unstructured) and is shown in Fig. 4.

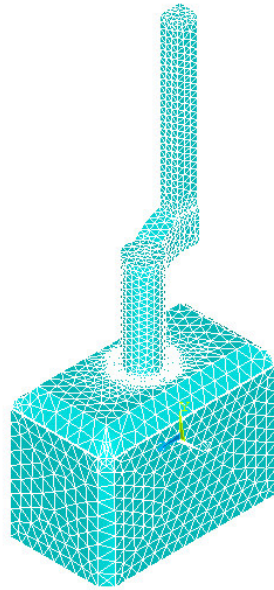


Figure 4. Finite element mesh used in the analysis.

3.4 BOUNDARY CONDITIONS

3.4.1 ELECTRICAL ANALYSIS

To take into account the symmetry of the problem, only one quarter of the electric current was applied as a boundary condition to the electrical problem. To distribute equally the current over the upper and lower surfaces of the system, the nodes of each surface were coupled. This is illustrated in Fig. 5. A perpendicular current density was then applied to these surfaces.

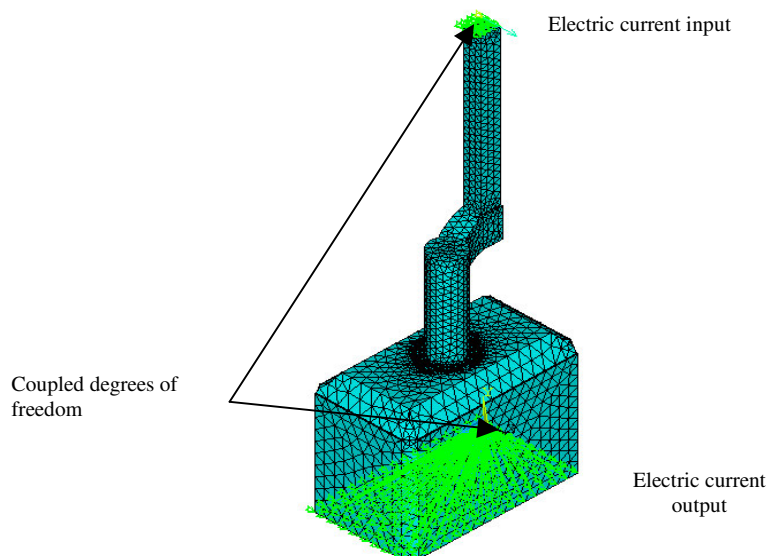


Figure 5. Coupling of nodes in the surfaces where electrical boundary conditions were considered.

3.4.2 THERMAL ANALYSIS

The boundary conditions were, in this case, the heat generated by Joule Effect calculated in the electric analysis and two reference temperatures measured by ALBRAS. This situation is illustrated in Fig. 6.

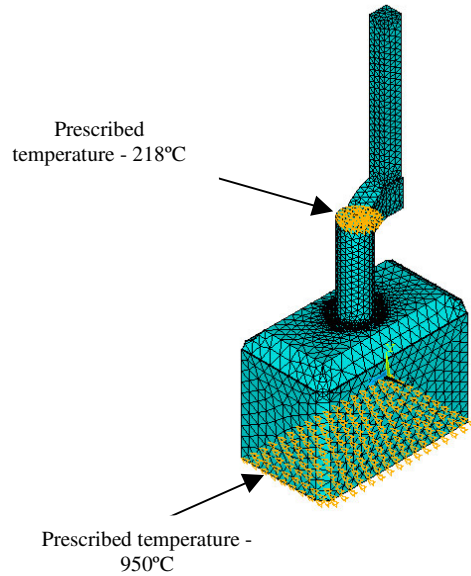


Figure 6. Example of temperature boundary conditions.

3.4.3. STRUCTURAL BOUNDARY CONDITIONS

The structural boundary conditions considered were the weight of the rod-anode set, the displacement restriction at the upper surface of the rod and the temperature gradients. The Fig. 7 shows these boundary conditions.

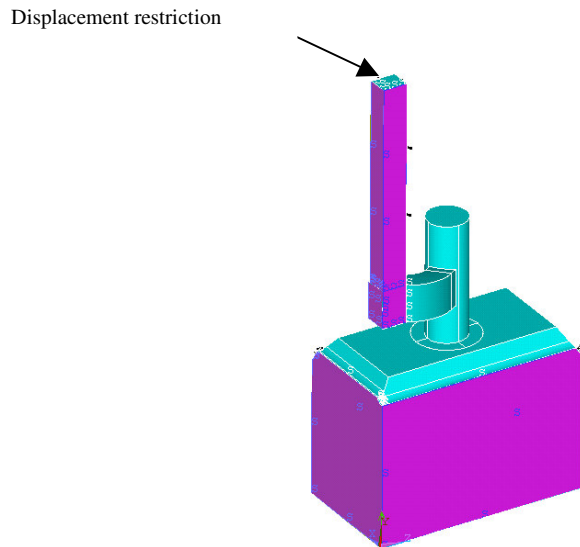


Figure 7. The shaded areas represent the applied surface boundary conditions.

4. RESULTS

The results of the finite element analysis are presented in the form of color maps showing the iso-surfaces of electric potential, temperature and mechanical stresses.

The Fig. 8 shows the electric potential distribution in Volts. It can be noted that the change in the potential is much more effective in the anode than in the rod region.

The temperature distribution is shown in the Fig. 9. The prescribed temperatures and the heat generated by the Joule effect are responsible for the verified pattern.

The figure 10 shows the heat generated by the Joule Effect in the hole, in the anode, that receives the rod.

The mechanical stresses are presented in the Figs. 11 to 13. The coupling is clearly a critical region concerning the these stresses.

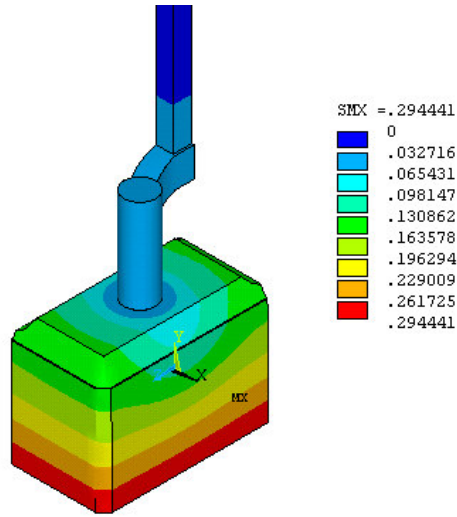


Figure 8. Colormap of the electric potential distribution in Volts.

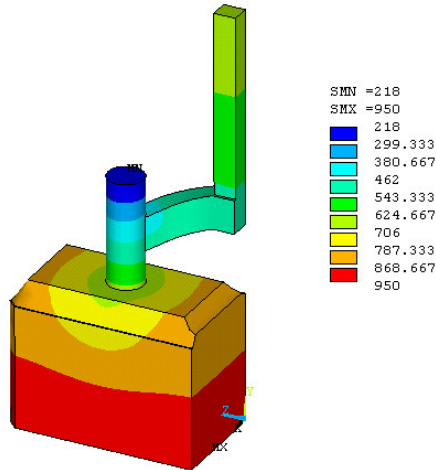


Figure 9. Colormap of the temperature distribution in Celsius degrees.

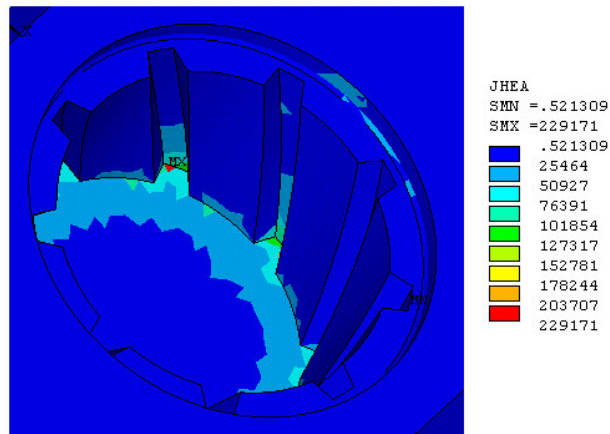


Figure 10. Detail of the colormap showing the heat loss by Joule Effect in the hole

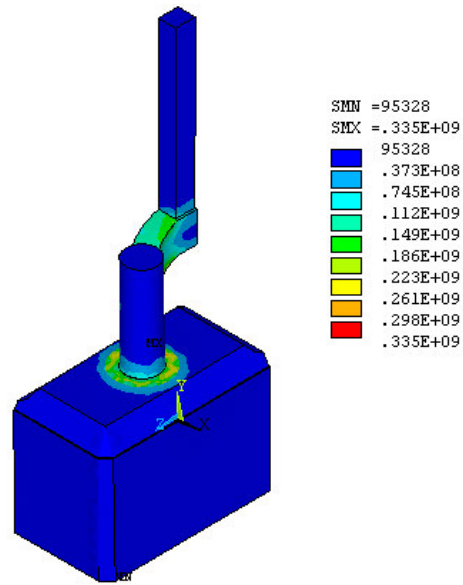


Figure 11. Colormap of the Von Mises Stresses in Pascal

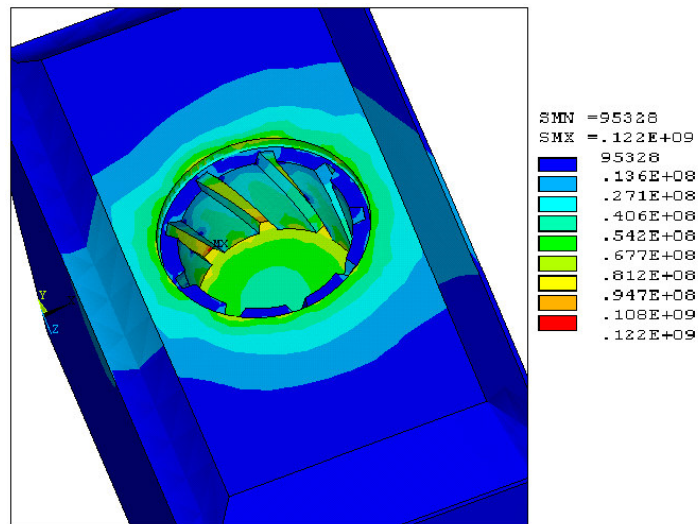


Figure 12. Colormap of the Von Mises Stresses around the hole, in Pascal

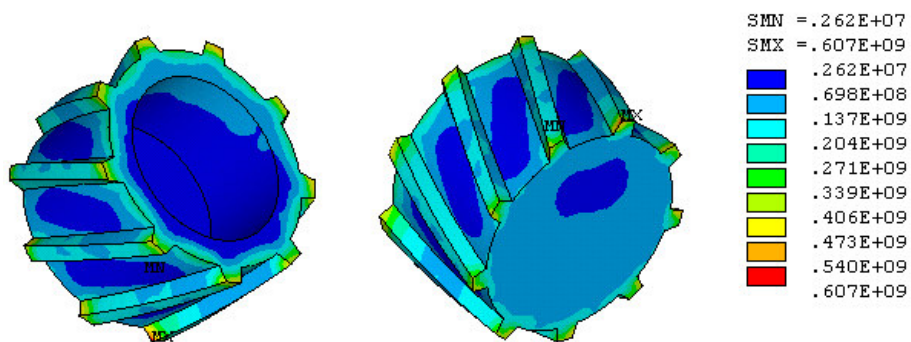


Figure 13. Colormap showing the Von Mises Stresses at the coupling

5. CONCLUSIONS

A direct coupling of the electrical, thermal and mechanical analysis was also done. The results were almost the same, but it was a lot more time consuming than the indirect approach.

The results obtained in this work can describe at least qualitatively the conditions verified in the rod-anode set. To obtain quantitative results, a more refined model and a calibration procedure are necessary.

It can be observed, in Fig. 8, that the electric potential loss in the rod is less than in the anode. This can be explained by the higher electrical resistance of the anode.

The Fig.10 shows that there is heat concentration at the edges of the helical grooves. This concentration occurs at the lower part of interface between the anode body and the rod. Changes in the geometry of this region could remove these point sources of heat and to improve the energy consumption in the process.

There is a stress concentration at the coupling rod-anode. The Figs. 12 and 13 show that this stress is concentrated at the edges of the grooves. An improvement of this characteristic can be obtained by a change in the form or in the number of grooves. However, this change must consider the electrical behaviour.

An optimisation procedure can be used to find the best shape and number for the grooves. The next step in this work is the sensitivity analysis of the rod-anode set to the changes discussed so far.

The authors would like to thank ALBRAS – Alumínio Brasileiro S.A. by the technical support to this work.

7. REFERENCES

- Assan, Aloísio Ernesto. Método dos Elementos Finitos: Primeiros Passos. 1ª edição. Campinas: Editora da Unicamp, 1999.
- Bathe, K.J. *Finite element procedures*. New Jersey: Prentice-Hall, 1996
- Batoz, J.L., Dhatt, G. Modélisation des structures par éléments finis. Volume 1: Solides Elastiques. Paris: Hermes, 1995.
- Cook, R.D., et al. Concepts and Applications of Finite Element Analysis, Third edition. New York : John Wiley and Sons , 1989.
- Dupuis, M. Computation of aluminum reduction cell energy balance using Ansys finite element models. Light Materials, 1998, p. 409-417
- Dupuis, M. Tabsh, I. Thermo-electric analysis of aluminum reduction cells. Proceedings of the 31ª Conference on Light Metal, 1992, p. 55-62
- Mangonon, P.L. The Principles of Materials Selection for Engineering Design. London: Prentice-Hall, 1999.
- Meier, M. W. Cracking Behaviour of Anodes. Sierre: R&D Carbon Ltd., 1996.
- Reddy, J. N. An Introduction To The Finite Element Method. New York: McGraw-Hill International Editions, 1984.
- Sherbinin, S.A. et al. 3D thermo-electric field modeling tool and its applications for energy regime simulations in aluminum reduction cells. Light Metals, 2000, p. 323-329
- Vogelsang, D. et al. From 110 to 175 kA: Retrofit of VAW Rheinwerk. Part I: Modernization Concept. Light Metals 1997.

8. COPYRIGHT NOTICE

The authors are the only responsible for the printed material included in his paper.